see commentary on page 1250

Autophagy in proximal tubules protects against acute kidney injury

Man Jiang[1], Qingqing Wei[1], Guie Dong[1], Masaaki Komatsu[2], Yunchao Su[3] and Zheng Dong[1,4]

[1]Department of Cellular Biology and Anatomy, Georgia Health Sciences University and Charlie Norwood VA Medical Center, Augusta, Georgia, USA; [2]Tokyo Metropolitan Institute of Medical Science, Setagaya-ku, Tokyo, Japan; [3]Department of Pharmacology and Toxicology, Georgia Health Sciences University and Charlie Norwood VA Medical Center, Augusta, Georgia, USA and [4]The Second Xiangya Hospital, Central South University, Changsha, China

Autophagy is induced in renal tubular cells during acute kidney injury; however, whether this is protective or injurious remains controversial. We address this question by pharmacologic and genetic blockade of autophagy using mouse models of cisplatin- and ischemia–reperfusion-induced acute kidney injury. Chloroquine, a pharmacological inhibitor of autophagy, blocked autophagic flux and enhanced acute kidney injury in both models. Rapamycin, however, activated autophagy and protected against cisplatin-induced acute kidney injury. We also established a renal proximal tubule–specific autophagy-related gene 7–knockout mouse model shown to be defective in both basal and cisplatin-induced autophagy in kidneys. Compared with wild-type littermates, these knockout mice were markedly more sensitive to cisplatin-induced acute kidney injury as indicated by renal functional loss, tissue damage, and apoptosis. Mechanistically, these knockout mice had heightened activation of p53 and c-Jun N terminal kinase, the signaling pathways contributing to cisplatin acute kidney injury. Proximal tubular cells isolated from the knockout mice were more sensitive to cisplatin-induced apoptosis than cells from wild-type mice. In addition, the knockout mice were more sensitive to renal ischemia–reperfusion injury than their wild-type littermates. Thus, our results establish a renoprotective role of tubular cell autophagy in acute kidney injury where it may interfere with cell killing mechanisms.

Kidney International (2012) **82,** 1271–1283; doi:10.1038/ki.2012.261; published online 1 August 2012

KEYWORDS: acute kidney injury; Atg7; autophagy; cisplatin; ischemia–reperfusion

Correspondence: *Zheng Dong, Department of Cellular Biology and Anatomy, Georgia Health Sciences University and Charlie Norwood VA Medical Center, 1459 Laney Walker Boulevard, Augusta, Georgia 30912, USA. E-mail: zdong@georgiahealth.edu*

Received 23 November 2011; revised 24 April 2012; accepted 24 May 2012; published online 1 August 2012

Acute kidney injury (AKI) induced by renal ischemia–reperfusion, sepsis, and nephrotoxins is a major kidney disease characterized by rapid loss of renal function, resulting in accumulation of metabolic wastes and imbalance of electrolytes and body fluid. Despite advances in basic research and medical care during the past several decades, clinical outcomes of AKI remain poor, with steadily increasing incidence, unacceptably high mortality, and unsatisfactory therapeutic approaches.[1,2] The pathogenesis of AKI is multiphasic and multifactorial, involving a complex interplay between renal tubules, vasculature, and inflammatory factors.[3–6] Pathologically, AKI is characterized by sublethal and lethal damage of renal tubules, resulting in tubular dysfunction and cell death in the forms of necrosis and apoptosis. In this regard, the tubular segments located within the outer stripe of out medulla, including proximal tubules, are especially susceptible to injury.[3–8]

Interestingly, in response to injury, renal tubular cells activate a myriad of defensive or cytoprotective mechanisms. For example, stress response genes, such as heat-shock proteins, are expressed by tubular cells to counteract the insult.[9] p21, a conventional cell cycle regulator, is upregulated in AKI to antagonize the cell death–promoting action of cyclin-dependent kinase 2.[5] More recently, macroautophagy (referred to as autophagy hereafter) has been demonstrated as a stress response of renal tubular cells to acute injury *in vitro* and *in vivo*. Whether autophagy is renoprotective or injurious remains very controversial.[10,11]

Autophagy is a cellular process of 'self-eating' whereby cytoplasmic components are sequestered into autophagic vesicles or vacuoles (called autophagosomes) and then delivered to lysosomes for degradation.[12,13] Recent research has delineated an evolutionarily conserved molecular machinery of autophagy, which includes a specific class of genes or proteins called autophagy-related genes, Atgs.[12,13] Atgs interact with each other and other regulatory proteins to form various protein complexes for the initiation, expansion, and final maturation of autophagosomes. Deficiency of a specific Atg leads to inhibition of relevant autophagic events. For example, Atg7 is a critical regulator of the Atg5–Atg12 and Atg8–phosphotidylethanolamine conjugation systems in autophagy.

Accordingly, these conjugations are attenuated in Atg7-null cells and tissues, resulting in complete blockade of autophagy.[14] Functionally, basal or physiological autophagy contributes to the maintenance of cellular homeostasis and quality control of proteins and subcellular organelles. In pathological conditions or cell stress, autophagy is induced and may serve as an adaptive and protective mechanism for cell survival; however, dysregulated autophagy may also contribute to cell death.[15,16] As a result, autophagy and its deregulation has been implicated in the pathogenesis of a variety of diseases such as cancer, neurodegeneration, and heart failure.[17]

In kidneys, autophagy is essential to the homeostasis and physiological function of podocytes.[18] Notably, autophagy induction has been demonstrated in renal tubular cells in experimental models of AKI induced by ischemia–reperfusion and nephrotoxicants such as cisplatin and cyclosporine.[19–26] Tubular autophagy was also detected following unilateral ureteral obstruction in mice.[27] Despite these reports, the mechanism of autophagy induction during AKI is unclear. Moreover, the role of autophagy in the pathogenesis of AKI remains to be debated. Although Chien *et al.*,[19] Suzuki *et al.*,[20] and Inoue *et al.*,[21] suggested a role of autophagy in tubular cell death,[5] we and others provided evidence for autophagy as a prosurvival, renoprotective mechanism in AKI.[22–25] Although the cause of the discrepancy is currently unknown, those studies concluded mainly based on the use of pharmacological inhibitors of autophagy. Nevertheless, the latest work by Kimura *et al.*[28] demonstrated heightened renal ischemia–reperfusion injury in proximal tubule–specific Atg5-knockout mice, providing the first genetic evidence for a renoprotective role in an AKI model. In the present study, we first examined the effect of chloroquine, a pharmacological inhibitor of autophagy, on cisplatin-induced AKI. We further established a renal proximal tubule–specific Atg7-knockout mouse model and demonstrated the high sensitivity of these mice to both cisplatin-induced AKI and renal ischemia–reperfusion-induced AKI. Mechanistically, Atg7-knockout kidney tissues showed heightened activation of p53 and c-Jun N-terminal kinase (JNK) during cisplatin treatment, the signaling pathways contributing to tubular cell death and AKI. In contrast to the aggravating effects of autophagy inhibition, activation of autophagy by rapamycin significantly attenuated cisplatin-induced renal injury. Together, these studies establish a renoprotective role of tubular cell autophagy in AKI.

RESULTS

Autophagy is induced in proximal tubules during cisplatin-induced AKI in C57BL/6 mice

We first confirmed the occurrence of autophagy in proximal tubular cells during cisplatin nephrotoxicity in C57BL/6 mice. As shown by immunoblot analysis of LC3 in Figure 1a, cisplatin led to a notable increase of LC3-II in renal cortical and outer medulla tissues, particularly at days 2 and 3. The LC3-II accumulation went down at day 4, possibly due to massive lysosomal degradation of the proteins in autophagosomes (autophagic flux). Morphologically, the formation of autophagosomes in kidneys was visualized by immunofluorescence staining of LC3. In control tissues, LC3 was diffusely distributed throughout the cells without punctated staining. Upon cisplatin treatment, intense dot-like LC3 staining puncta appeared in some renal tubular cells of renal cortex and outer medulla, indicating the formation of autophagosomes (Figure 1b, LC3). The localization of LC3 puncta was further determined by costaining with either fluorescein isothiocyanate (FITC)–labeled phaseolus vulgaris agglutinin (PHA) or peanut agglutinin, the two lectins that bind proximal and distal tubular cells, respectively.[29] Most of the LC3 puncta colocalized with the FITC-PHA-positive renal tubules, suggesting that autophagy was induced mainly in proximal tubular cells by cisplatin (Figure 1b, FITC-PHA and merge). Quantitatively, on average, approximately three LC3 dots per proximal tubule were found in the cisplatin-treated mice, whereas no LC3 dot was observed in the control mice (Figure 1c). By electron microscopy, our previous work detected the formation of autophagic vacuoles in proximal tubule cells during cisplatin-induced AKI in mice. Together, these results demonstrate compelling evidence for the occurrence of autophagy in this AKI model.

Inhibition of autophagy by chloroquine worsens cisplatin-induced AKI in C57BL/6 mice

The role of autophagy in the pathogenesis of AKI remains controversial.[19–25] To address this question, we initially tested the effects of chloroquine, a pharmacological inhibitor of autophagy, on cisplatin-induced AKI in C57BL/6 mice. Suppression of autophagic flux by chloroquine was first confirmed by immunoblot analysis of LC3 and p62. As shown in Figure 2a and b, at day 4 of cisplatin treatment, LC3-II induction was not as obvious as the earlier time points of days 2 and 3, probably owing to autolysosomal degradation. Chloroquine blocked the lysosomal degradation of LC3 in autophagosomes, leading to a marked accumulation of LC3-II following cisplatin treatment. As a selective substrate of autophagy, p62 degradation was also inhibited by chloroquine (Figure 2a and b), further confirming the inhibitory effect of chloroquine on autophagy in kidney tissues. We then examined cisplatin-induced AKI in the absence or presence of chloroquine. Cisplatin at 25 mg/kg induced moderate AKI within 3 days as indicated by blood urea nitrogen (BUN) measurement, which was not affected by chloroquine. At day 4 of cisplatin treatment, BUN level increased to 90 mg/dl, which was aggravated to 181 mg/dl by chloroquine (Figure 2c). Similarly, serum creatinine was increased from 0.84 to 1.54 mg/dl by chloroquine at day 4 of cisplatin treatment (Figure 2d). Consistent with the functional data, cisplatin-induced tissue damage in renal cortex and outer medulla was aggravated by chloroquine (Figure 2e). Cisplatin treatment led to the loss of brush border, tubular dilation and distortion, and cell lysis in some proximal tubules. In the presence of chloroquine, the majority of the tubules were injured and the severity of the injury was also increased, showing tubular disruption and massive tubular lysis with sloughed debris in

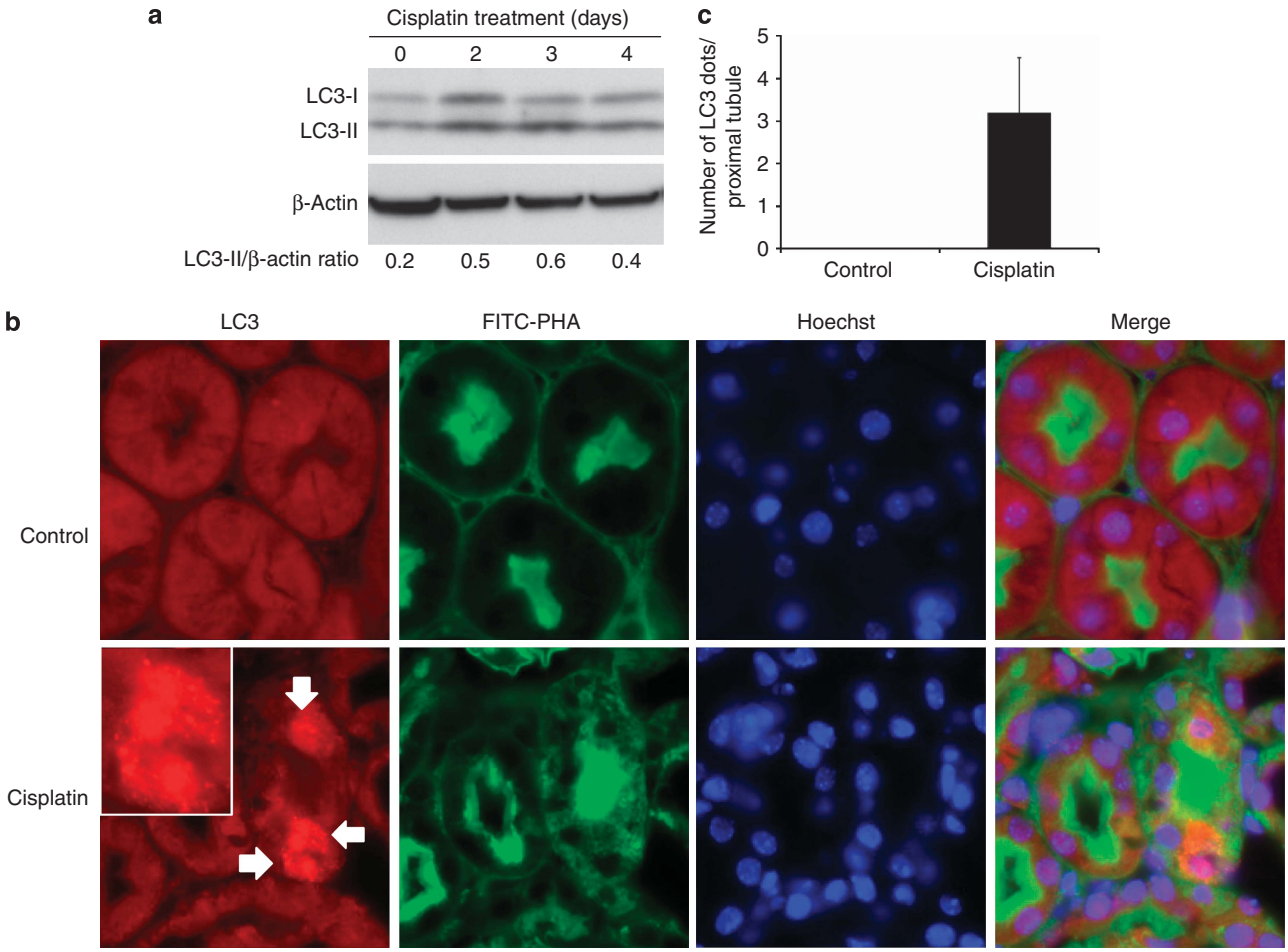

Figure 1 | Autophagy is induced in proximal tubules during cisplatin nephrotoxicity in C57BL/6 mice. C57BL/6 mice (male, 8–10 weeks old) were injected with 25 mg/kg cisplatin or saline as control. (**a**) After the indicated time points, kidneys were harvested to collect cortical and outer medulla tissues for immunoblot analysis of LC3 and β-actin (loading control). For densitometry, the LC3-II signals were divided by the β-actin signal of the same samples to determine the ratios. (**b**) At 3 days after treatment, kidneys were collected for immunofluorescence staining of LC3, fluorescein isothiocyanate (FITC)–labeled phaseolus vulgaris agglutinin (PHA), and Hoechst 33342 (original magnification × 630). Arrows point to LC3 puncta (autophagosomes) and insets show LC3 puncta at a higher magnification. (**c**) Quantification of LC3 dots in individual proximal tubule of the cisplatin-treated group. Data are expressed as mean ± s.d. Control tissues did not show LC3 dots.

the lumen. Semiquantification confirmed that chloroquine significantly increased kidney tissue damage during cisplatin treatment (Figure 2f: 1.3 for cisplatin vs. 2.9 for cisplatin + chloroquine). Further examination of renal tissues by TUNEL (TdT-mediated dUTP nick-end labeling) assay showed that cisplatin-induced tubular cell apoptosis was increased by chloroquine (Figure 2g and h). As a control, chloroquine alone did not induce kidney injury in C57BL/6 mice (data not shown). Collectively, these results demonstrate the inhibitory effect of chloroquine on cisplatin-induced autophagy and the aggravating effect of chloroquine on AKI, suggesting a renoprotective role of autophagy in this disease model.

Creation and characterization of proximal tubule–specific Atg7-knockout mouse model

To further define the role of tubular cell autophagy in AKI, we established a conditional knockout mouse model, in which Atg7 was deleted specifically from renal proximal tubules in kidneys. Atg7 is critical for the conjugation events in autophagy.[30] Mice bearing the floxed Atg7 alleles ($Atg7^{flox/flox}$) were generated by inserting two loxP sites around exon 14 that encodes the active site cysteine essential for activation of the conjugation substrates.[14] $Atg7^{flox/flox}$ mice were bred to transgenic mice expressing the Cre recombinase under the control of a modified PEPCK promoter (PEPCK-Cre) that directs Cre expression predominantly in kidney proximal tubular cells and marginally in hepatocytes.[31] After the first round of breeding, heterozygous female progenies ($Atg7^{flox/+}X^{cre}X$) were obtained and then crossed with $Atg7^{flox/flox}$ males to generate $Atg7^{flox/flox}X^{cre}Y$ mice with PEPCK-Cre-mediated Atg7 deletion from renal proximal tubules (PT-Atg7-KO, Figure 3a). As PEPCK-Cre is linked to X chromosome,[31] we only used male mice for the study to ensure correct genotypes.

To verify the genotypes, three sets of PCR were conducted for the genomic DNA sample of each mouse. The genotype of

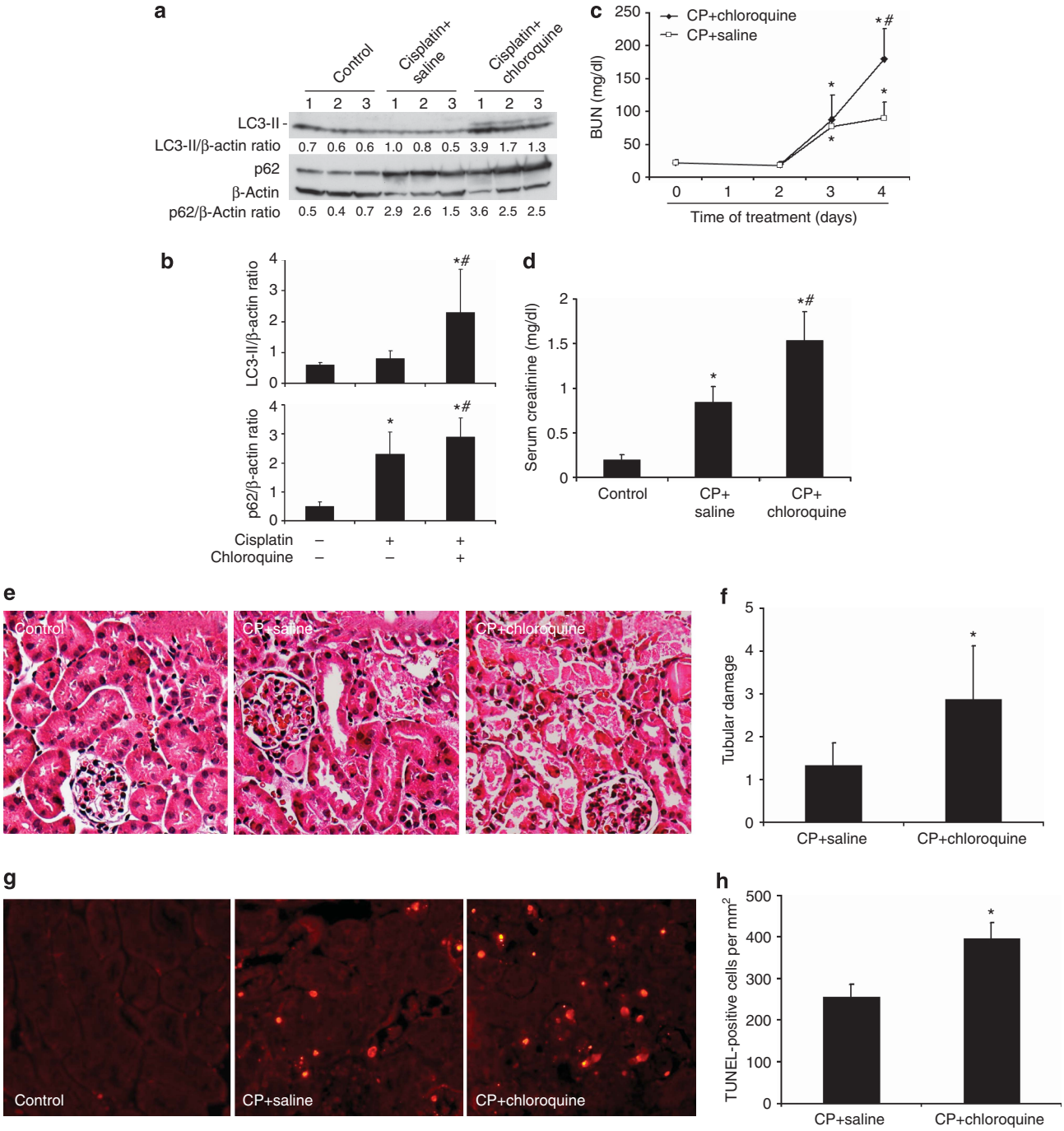

Figure 2 | Inhibition of autophagy by chloroquine worsens cisplatin-acute kidney injury (AKI) in C57BL/6 mice. C57BL/6 mice (male, 8–10 weeks old, littermates or age-matched nonlittermates) were divided into three groups for the following treatments, respectively: (1) saline control ($n = 3$); (2) cisplatin + saline ($n = 4$); and (3) cisplatin + chloroquine ($n = 5$). The mice were killed on day 4. (**a**) Whole-tissue lysate of kidney cortex was collected for immunoblot analysis of LC3, p62, and β-actin. (**b**) Densitometry of LC3-II and p62 signals. The blot in **a** was analyzed by densitometry. The LC3-II and p62 signals were divided by the β-actin signal of the same samples to determine the ratios. Data are expressed as mean ± s.d. $^{*}P < 0.05$, significantly different from the control group; $^{\#}P < 0.05$, significantly different from the cisplatin + saline group. (**c**, **d**) Blood samples were collected for measurements of blood urea nitrogen (BUN) and serum creatinine levels. Data are expressed as mean ± s.d. $^{*}P < 0.05$, significantly different from the control (or day 0) group; $^{\#}P < 0.05$, significantly different from the cisplatin (CP) + saline group. (**e**) Representative histology of kidney cortex (hematoxylin–eosin (H–E) staining, original magnification × 200). (**f**) Pathological score of tubular damage in cisplatin + saline and cisplatin + chloroquine groups. (**g**) Representative images of TUNEL (TdT-mediated dUTP nick-end labeling) staining (original magnification × 200). (**h**) Quantification of TUNEL-positive cells in cisplatin + saline and cisplatin + chloroquine groups. Data in **f** and **h** are expressed as mean ± s.d. $^{*}P < 0.05$, significantly different from the cisplatin + saline group. Control tissues without cisplatin treatment did not show tubular damage or apoptotic cells.

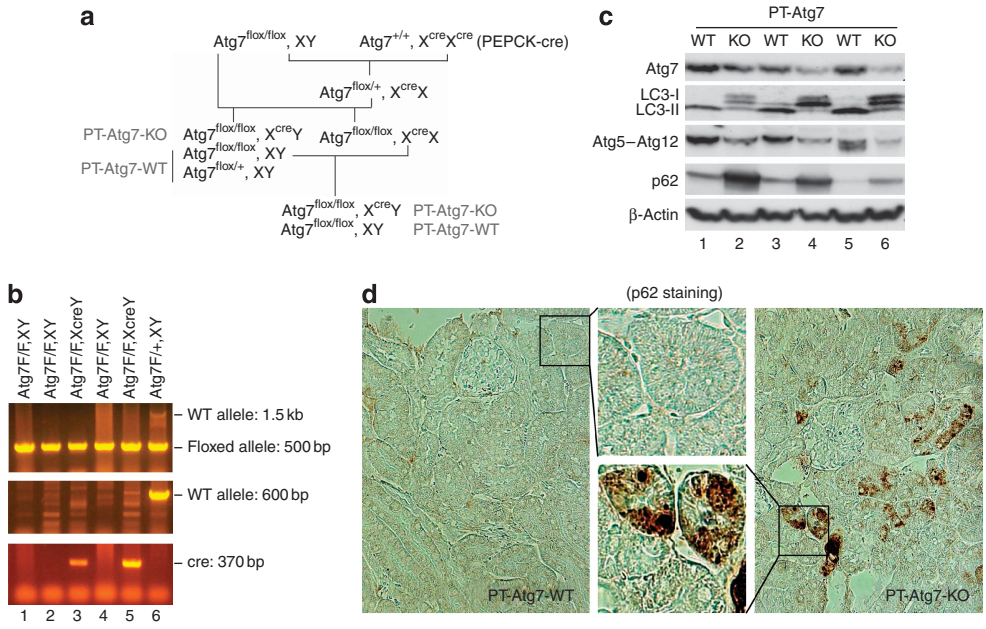

Figure 3 | Creation and characterization of the PT-Atg7-KO mouse model. (**a**) Breeding protocol for generating PT-Atg7-KO mice. Male littermate mice of 8–9 weeks old were used for experiments after genotypes were confirmed. (**b**) Representative images of PCR-based genotyping. Genomic DNA was extracted from tail biopsy and amplified to detect wild-type (WT) and floxed alleles of Atg7 and PEPCK-Cre allele as indicated. (**c**) Whole-tissue lysate of kidney cortex was collected from PT-Atg7-KO and wild-type (PT-Atg7-WT) littermate mice for immunoblot analysis of Atg7, LC3, Atg5 (Atg12 conjugated), p62, and β-actin. (**d**) Immunohistochemical staining of p62 (original magnification × 200) in kidney cortical tissues of wild-type and PT-Atg7-KO mice. The selected areas were shown at high magnification in the middle panels.

PT-Atg7-KO mice was indicated by the amplification of the ~500-bp fragment of the floxed allele, the nonamplification of the ~600-bp fragment of the wild-type allele, and the amplification of the ~370-bp fragment of the Cre gene (Figure 3b, lanes 3 and 5). The absence of the Cre gene ensured the genotype of wild-type (PT-Atg7-WT) mice (Figure 3b, lanes 1, 2, 4, and 6). By immunoblot analysis of the tissues from kidney cortex and outer medulla that consist mainly of proximal tubules, we confirmed that Atg7 expression was indeed reduced in PT-Atg7-KO mice, compared with their wild-type littermates (Figure 3c for littermate tissue comparison: lanes 2 vs. 1, 4 vs. 3, and 6 vs. 5). We further verified the PT-Atg7-KO model functionally. To this end, we first analyzed the Atg7-mediated autophagic conjugations in collected kidney tissues. In wild-type tissues, LC3-II, the phosphatidylethanolamine-conjugated form of LC3, was mainly detected (Figure 3c, lanes 1, 3, and 5); however, in PT-Atg7-KO tissues, large amount of LC3-I accumulated, whereas LC3-II was barely detectable (Figure 3c, lanes 2, 4, and 6). Furthermore, wild-type kidney tissues showed high levels of Atg5–Atg12 conjugation, which was markedly reduced in PT-Atg7-KO tissues (Figure 3c, lanes 1, 3, and 5 vs. lanes 2, 4, and 6). In addition, we examined kidney tissues for the expression and localization of p62, a selective substrate of autophagy. Immunoblot analysis demonstrated markedly higher p62 in PT-Atg7-KO kidney tissues than wild type (Figure 3c, lanes 2, 4, and 6 vs. lanes 1, 3, and 5). By immunohistochemistry, positive p62 staining was detected in PT-Atg7-KO kidney tissues, and not in wild-type tissues (Figure 3d). Notably, p62 staining in PT-Atg7-KO tissues appeared as unevenly distributed cytoplasmic puncta of various sizes, characteristic of the inclusion bodies seen in autophagy-deficient cells.[32] By morphology, the p62 staining appeared exclusively in proximal tubules. It is noteworthy that p62 staining did not show a general increase in all proximal tubular cells, suggesting that the basal level of autophagy varies in different tubular cells. Together, these studies validate the PT-Atg7-KO model, in which Atg7 is specifically deleted from proximal tubular cells in kidneys.

Cisplatin-induced autophagy is inhibited in renal proximal tubules in PT-Atg7-KO mice

After verifying the autophagic defects in proximal tubules of PT-Atg7-KO mice under unchallenged conditions, we further examined autophagy during cisplatin treatment. As shown in Figure 4a, in response to cisplatin treatment, wild-type kidney tissues showed LC3-II accumulation, whereas the conversion of LC3-I to LC3-II was completely abrogated in PT-Atg7-KO kidneys. Atg5–Atg12 conjugation was also reduced in PT-Atg7-KO tissues. Consistent with Figure 3, the basal level of p62 was significantly higher in PT-Atg7-KO tissues than wild-type tissues, and following cisplatin treatment p62 increased markedly (Figure 4a, PT-Atg7-KO). The effect of Atg7 deficiency on cisplatin-induced autophagy in proximal tubules was then determined morphologically by coimmunostaining of LC3 and FITC-labeled PHA. As shown

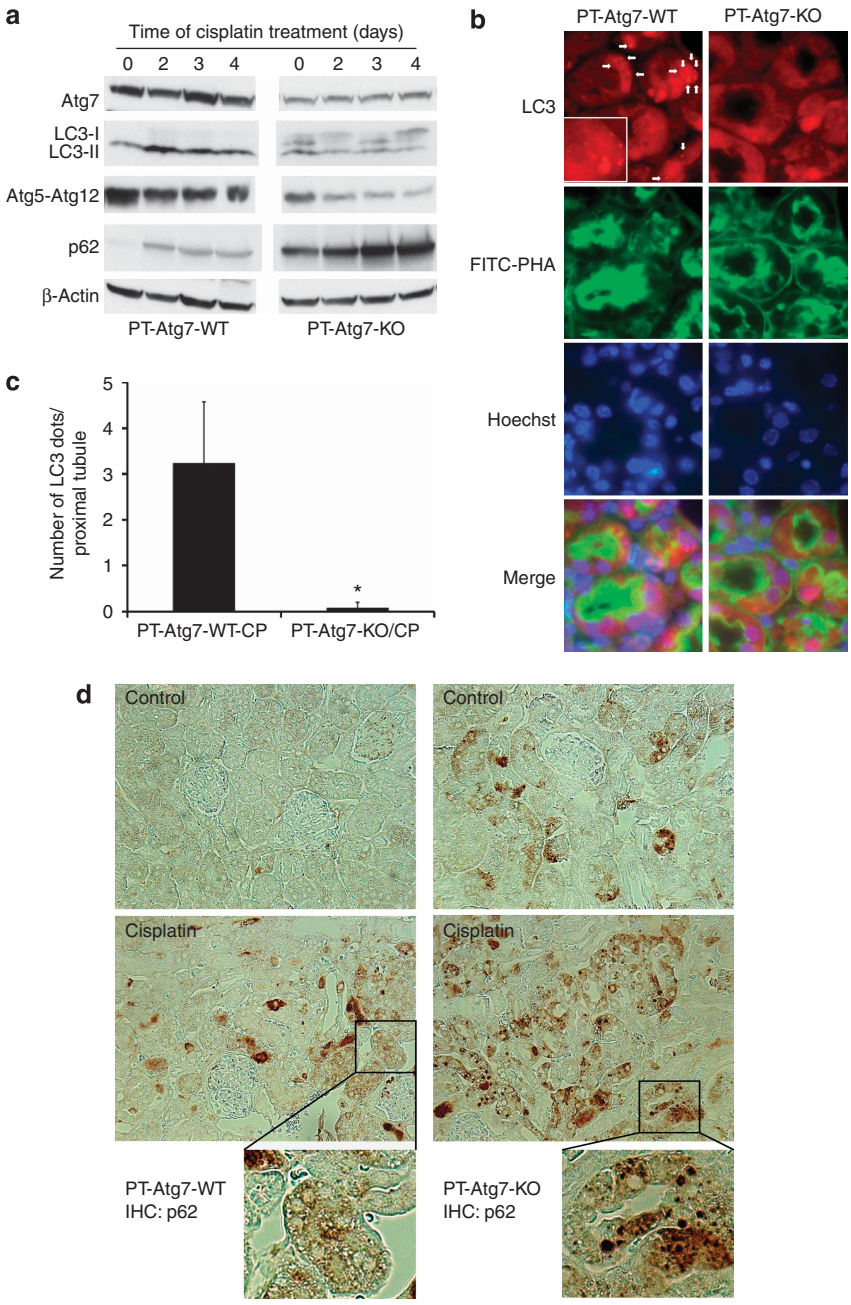

Figure 4 | Cisplatin-induced autophagy is inhibited in renal proximal tubules in PT-Atg7-KO mice. Wild-type and PT-Atg7-KO mice were injected with 25 mg/kg cisplatin or saline as control. (**a**) After the indicated time points, kidneys were harvested to collect cortical tissues for immunoblot analysis of Atg7, LC3, Atg5 (Atg12 conjugated), p62, and β-actin. (**b**) At 3 days after injection, kidneys were collected for immunofluorescence staining of LC3, fluorescein isothiocyanate (FITC)-labeled phaseolus vulgaris agglutinin (PHA), and Hoechst 33342 (original magnification $\times 630$). Representative images of cisplatin-treated wild-type and PT-Atg7-KO groups were shown. Arrows point to LC3 dots (autophagosomes) and inset shows LC3 dots at higher magnifications. (**c**) Quantification of LC3 dots in individual proximal tubule of cisplatin-treated wild-type and PT-Atg7-KO groups. Data are expressed as mean ± s.d. $^*P < 0.05$, significantly different from the wild-type group. (**d**) After 4 days of treatment, kidneys were collected for immunohistochemical staining of p62 (original magnification $\times 200$). The selected areas are shown at high magnifications.

in Figure 4b, punctuate or granular LC3 staining was detected in some proximal tubular cells of wild-type kidneys during cisplatin treatment, which was barely seen in PT-Atg7-KO tissues. The number of LC3 puncta per proximal tubule was significantly reduced from 3.2 in wild-type mice to 0.1 in PT-Atg7-KO tissues (Figure 4c). By immunohistochemistry, we found that, compared with the control, cisplatin induced massive p62 accumulation in proximal tubules in PT-Atg7-KO mice, as indicated by remarkably increased amount and size of cytoplasmic p62 inclusion bodies (Figure 4d, high-magnification inserts). In wild-type tissues, there was an increase in p62 staining in some proximal tubular cells after

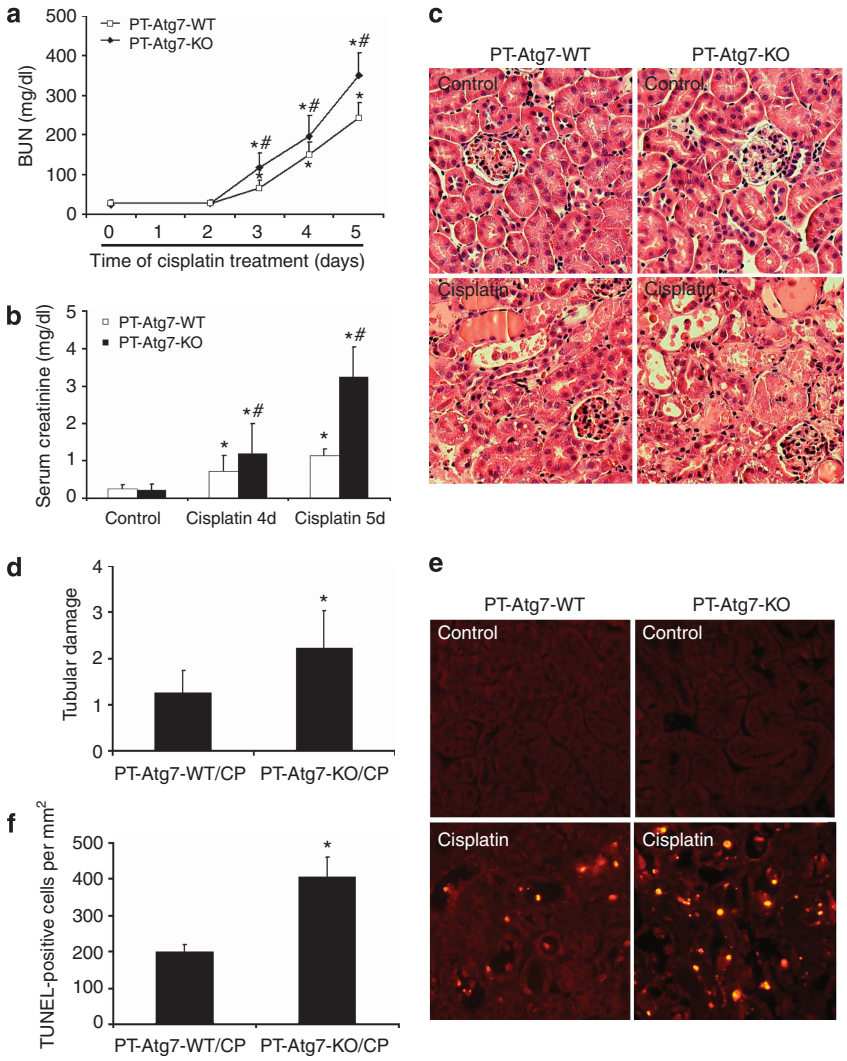

Figure 5 | Cisplatin-acute kidney injury (AKI) is aggravated in PT-Atg7-KO mice. Wild-type ($n = 15$) and PT-Atg7-KO littermate mice ($n = 21$) were injected with 25 mg/kg cisplatin or saline as control. (**a**, **b**) Blood samples were collected for measurements of blood urea nitrogen (BUN) and serum creatinine levels. Data are expressed as mean ± s.d. $^{*}P < 0.05$, significantly different from the control (or day 0) groups; $^{\#}P < 0.05$, significantly different from the relevant wild-type group. (**c**) Representative histology of kidney cortex (hematoxylin–eosin (H–E) staining, original magnification × 200). (**d**) Pathological score of tubular damage in cisplatin-treated wild-type and PT-Atg7-KO mice. (**e**) Representative images of TUNEL (TdT-mediated dUTP nick-end labeling) staining (original magnification × 200). (**f**) Quantification of TUNEL-positive cells in cisplatin-treated wild-type and PT-Atg7 KO groups. Data in **d** and **f** are expressed as mean ± s.d. $^{*}P < 0.05$, significantly different from the wild-type group.

cisplatin treatment, but in general the staining was diffuse and not indicative of inclusion bodies (Figure 4d). Together, these results suggest that cisplatin-induced autophagy is suppressed in renal proximal tubular cells in PT-Atg7-KO mice.

Cisplatin-induced AKI is aggravated in PT-Atg7-KO mice

By using the PT-Atg7-KO model, we then determined the role of autophagy on cisplatin-induced AKI. Without treatment, both PT-Atg7-KO mice and their wild-type littermates showed similarly low levels of BUN and serum creatinine, indicating normal renal function. At 4 days after cisplatin injection, wild-type mice developed moderate renal failure, with BUN and serum creatinine levels increased to 151 and 0.74 mg/dl, respectively. In the same experiments, PT-Atg7-KO mice had more severe loss of renal function, showing BUN level of 198 mg/dl and serum creatinine level of 1.21 mg/dl (Figure 5a and b). Notably, the progression of AKI was accelerated thereafter in PT-Atg7-KO mice. At 5 days after cisplatin treatment, these mice had 351 mg/dl BUN and 3.24 mg/dl serum creatinine levels, whereas their wild-type littermates had 244 mg/dl BUN and 1.15 mg/dl serum creatinine levels (Figure 5a and b). Histological analysis confirmed that, compared with wild type, cisplatin induced much more severe kidney tissue damage in PT-Atg7-KO mice, which showed widespread, extensively damaged proximal tubules in the renal cortex and outer medulla (Figure 5c). These tissues had a tubular damage score of 2.2, whereas the score was 1.3 for wild-type tissues (Figure 5d). Further

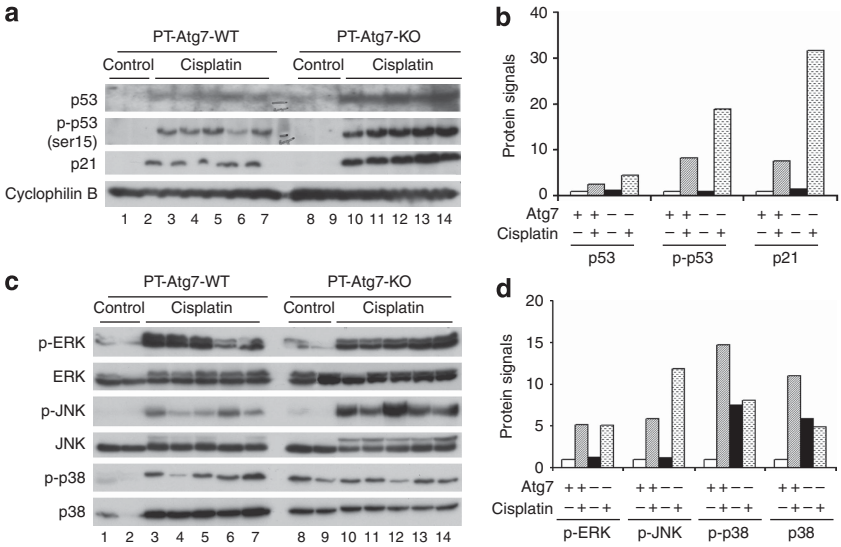

Figure 6 | Heightened p53 and c-Jun N-terminal kinase (JNK) activation during cisplatin-acute kidney injury (AKI) in PT-Atg7-KO mice. Wild-type and PT-Atg7-KO littermate mice were injected with 25 mg/kg cisplatin ($n = 8$ for wild-type and PT-Atg7-KO, respectively) or saline as control ($n = 5$ for wild-type and PT-Atg7-KO, respectively). After 4 days of treatment, whole-tissue lysate of renal cortex and outer medulla was collected for immunoblot analysis. (**a**) Representative blots of p53, p-p53 (ser15), and p21. Cyclophilin B was used as a loading control. (**b**) Densitometry of p53, p-p53 (ser15), and p21 signals. (**c**) Representative blots of phosphorylated extracellular signal–regulated kinase (p-ERK), ERK, phosphorylated (p)-JNK, JNK, phosphorylated (p)-p38, and p38. (**d**) Densitometry of p-ERK, p-JNK, p-p38, and p38 signals. For densitometric analysis in **b** and **d**, the protein signal of the wild-type control group (average value of 5 mice) was arbitrarily set as 1, and the signals of other conditions (average value for each condition) were normalized.

examination by TUNEL assay indicated that cisplatin induced significantly more apoptosis in kidney tissues of PT-Atg7-KO mice than wild-type littermates (Figure 5e and f). Together with the results of the chloroquine effect (Figure 2), these studies demonstrate compelling evidence for a renoprotective role of autophagy against cisplatin-induced AKI.

Heightened p53 and JNK activation during cisplatin treatment in PT-Atg7-KO mice

The pathogenesis of cisplatin-AKI is very complex, involving tubular damage, vascular alteration, and a rapid and lasting inflammatory response.[4,5,33] The intrinsic mechanism of tubular cell death involves the activation of and interplay between multiple signaling pathways including p53 and mitogen-activated protein kinases.[4,5,34] To gain initial insights into the mechanisms by which autophagy protects renal tubular cells, we first determined whether p53 signaling was affected in Atg7-deficient mice. Consistent with previous reports,[35,36] cisplatin induced p53 accumulation and phosphorylation in kidney tissues in wild-type mice (Figure 6a, lanes 1–7). Notably, significantly higher p53 activation was demonstrated in PT-Atg7-KO tissues (Figure 6a, lanes 8–14). In line with this observation, the induction of p21 (a transcription target of p53) was induced by cisplatin in wild-type tissues, and the induction was much more pronounced in PT-Atg7-KO tissues (Figure 6a). Densitometric analysis showed that cisplatin induced 2.6- and 8-fold increases in total and phosphorylated p53 in wild-type kidney tissues, and 4.5- and 20-fold increases in PT-Atg7-KO tissues, respectively (Figure 6b). The results suggest that autophagy may interfere with p53 activation during cisplatin-AKI. It is noteworthy that p21 is induced in AKI as a defensive mechanism for kidney protection,[5] and the induction is often positively correlated with the severity of AKI. Consistently, in our study, cisplatin induced much more severe AKI and markedly higher p21 in PT-Atg7-KO mice than that in wild-type mice.

We further determined the effect of autophagy deficiency on mitogen-activated protein kinases, another important signaling pathway in cisplatin-AKI.[4,5] Cisplatin induced similar levels of extracellular signal–regulated kinase phosphorylation in wild-type and PT-Atg7-KO kidney tissues (Figure 6c and d). However, JNK phosphorylation was induced to higher levels in PT-Atg7-KO kidney tissues than wild-type tissues (Figure 6c and d). Interestingly, the changes of p38 were detected at both phosphorylation and total protein levels. PT-Atg7-KO kidney tissues showed higher total p38 expression than wild-type tissues. After cisplatin treatment, there was a consistent increase of total p38 in wild-type, but not PT-Atg7-KO, tissues (Figure 6c, p38). Similarly, phosphorylated p38 was higher in PT-Atg7-KO tissues under control condition, and after cisplatin treatment p-p38 increased in wild-type tissues but not in PT-Atg7-KO tissues. The results suggest that autophagy may affect mitogen-activated protein kinases, especially JNK, to protect against cisplatin-AKI.

Increased sensitivity of Atg7-deficient proximal tubular cells to cisplatin-induced apoptosis

To complement the *in vivo* study, we examined cisplatin-induced apoptosis in primary cultures of proximal tubular

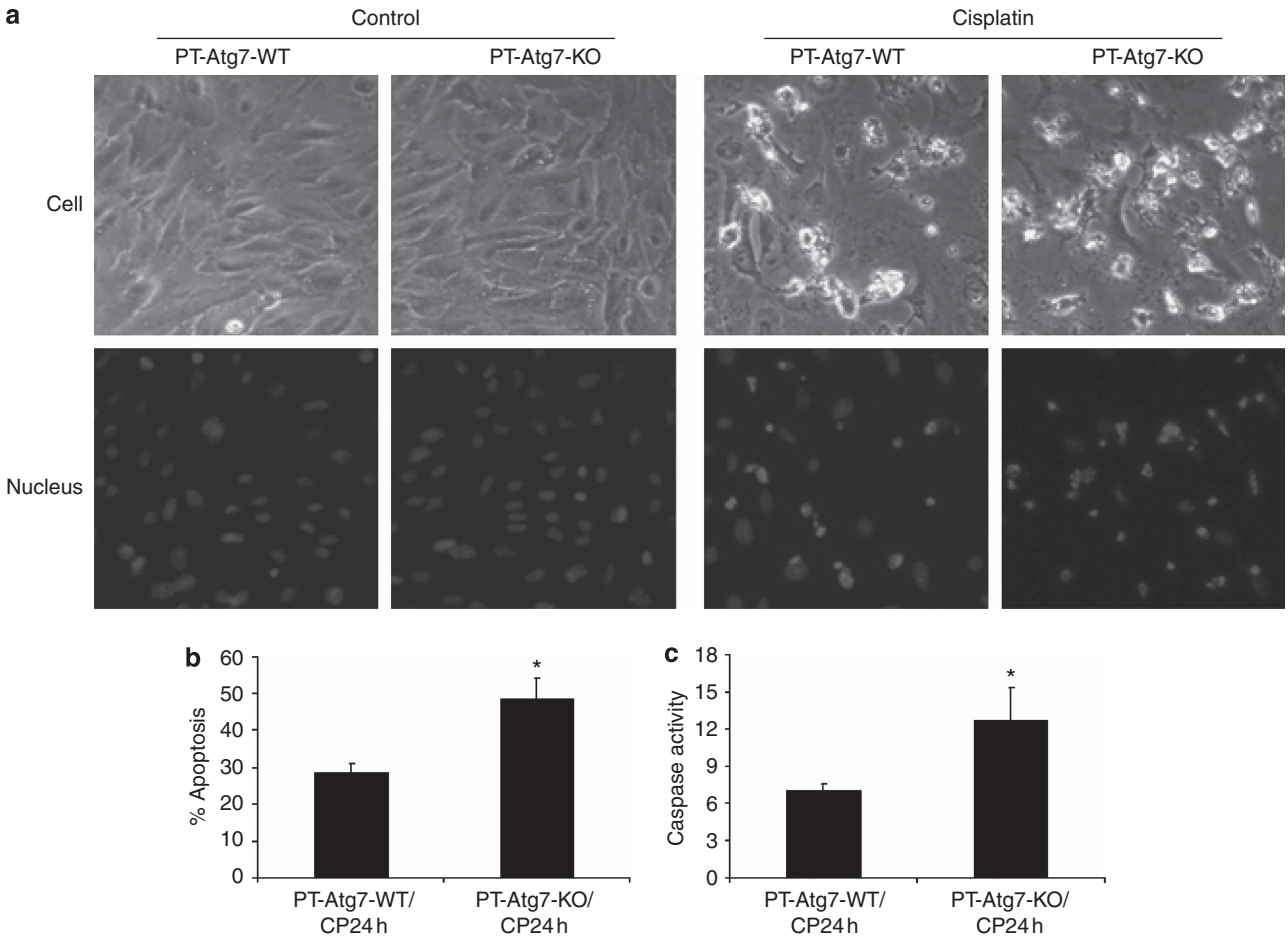

Figure 7 | Proximal tubular cells isolated from PT-Atg7-KO mice are sensitized to cisplatin-induced apoptosis. Primary proximal tubular cells isolated from wild-type and PT-Atg7-KO mice were treated with 30 μmol/l cisplatin for 24 h. Apoptosis was assessed by cell morphology and caspase activation. (**a**) Representative cell and nuclear morphology (original magnification × 200). After treatment, cells were stained with Hoechst 33342 to record cell and nuclear morphology. (**b**) Apoptosis percentage. Apoptotic cells were counted to determine the percentage of apoptosis. (**c**) Caspase activity measured by enzymatic assays using carbobenzoxy-Asp-Glu-Val-Asp-7-amino-4-trifluoromethyl coumarin as substrates. Data in **b** and **c** are expressed as mean ± s.d. *$P < 0.05$, significantly different from the wild-type group.

cells isolated from PT-Atg7-KO and wild-type mice. As shown in Figure 7a, apoptosis was minimal under control conditions regardless of the status of Atg7. After 24 h of cisplatin treatment, some cells underwent apoptosis, showing the typical morphological changes including cellular shrinkage, and formation of apoptotic bodies (Figure 7a, upper panels). Nuclear staining with Hoechst 33342 also showed nuclear condensation and fragmentation in these cells (Figure 7a, lower panels). Importantly, apoptosis was obviously higher in Atg7-KO tubular cells (Figure 7a). Quantification by cell counting showed that cisplatin induced ~28% apoptosis in wild-type cells, but ~49% in Atg7-KO cells (Figure 7b). The morphological results were confirmed by caspase activity measurement. As shown in Figure 7c, caspase activation induced by cisplatin was increased from 7.1 nmol/mg/h in wild-type cells to 12.7 nmol/mg/h in Atg7-KO cells. Thus, proximal tubular cells isolated from PT-Atg7-KO mice were more sensitive to cisplatin-induced apoptosis, further supporting the *in vivo* study for a renoprotective role of autophagy.

PT-Atg7-KO mice are more sensitive to ischemic AKI

Although this study focused on cisplatin-induced kidney injury, our previous work using pharmacological autophagy inhibitors[22] and the latest study by Kimura *et al.*[28] using a proximal tubule–specific Atg5-knockout mouse model have suggested that autophagy is renoprotective in ischemic AKI. We further verified these findings using the PT-Atg7-KO model. To this end, 25 min of bilateral renal ischemia was induced in PT-Atg7-KO mice and their wild-type littermates. AKI was monitored by measuring BUN and serum creatinine levels at different time points of reperfusion. As shown in Figure 8a, at 24 h following reperfusion, PT-Atg7-KO mice had the BUN level of 110 mg/dl, which was significantly higher than the BUN level of 84 mg/dl in wild-type mice. It is noteworthy that 25 min of ischemia induced moderate AKI that was reversible, and as a result both wild-type and PT-Atg7-KO mice displayed recovery of renal function after initial injury. On 72 h of reperfusion, BUN level went down to 54 mg/dl in wild-type mice, whereas PT-Atg7-KO mice

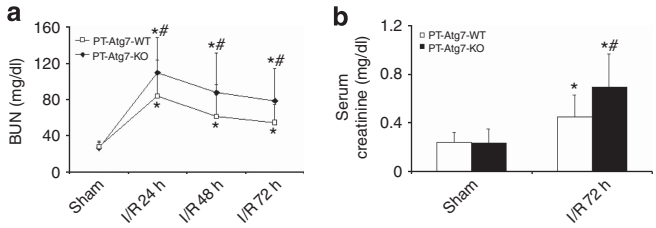

Figure 8 | PT-Atg7 KO mice are more sensitive to renal ischemia–reperfusion (I/R) injury. Wild-type ($n = 14$) and PT-Atg7-KO littermate mice ($n = 14$) were subjected to sham operation or 25 min of bilateral renal ischemia followed by 0–72 h of reperfusion. Blood samples were collected for measurements of (**a**) blood urea nitrogen (BUN) and (**b**) serum creatinine levels. Data are expressed as mean ± s.d. $^{*}P < 0.05$, significantly different from the sham control groups; $^{\#}P < 0.05$, significantly different from the wild-type group.

maintained BUN level at a higher level of 79 mg/dl (Figure 8a). Consistently, PT-Atg7-KO mice also showed significantly higher serum creatinine level at 72 h of reperfusion than their wild-type littermates (Figure 8b). Therefore, both cisplatin- and ischemia–reperfusion-induced AKI were aggravated in PT-Atg7-KO mice, demonstrating a renoprotective role of tubular autophagy in AKI.

Activation of autophagy by rapamycin reduces cisplatin-induced AKI in C57BL/6 mice

To complement the autophagy inhibitory studies, we tested the effects of autophagy activation on cisplatin-induced AKI in C57BL/6 mice. First, we examined whether rapamycin, a pharmacological inhibitor of the mammalian target of rapamycin, could enhance autophagy in kidneys during cisplatin treatment. As shown in Figure 9a, LC3-II increased in renal cortical tissues 2 days after cisplatin injection. This accumulation was further increased by rapamycin, suggesting an enhancement of cisplatin-induced autophagy. We then compared renal function loss and tissue damage in the absence and presence of rapamycin. Cisplatin led BUN level to increase to 168 mg/dl at day 4, which was partially but significantly reduced to 133 mg/dl by rapamycin (Figure 9b). Serum creatinine was also decreased from 1.06 mg/dl in the cisplatin-treated mice to 0.76 mg/dl in the mice treated with cisplatin + rapamycin (Figure 9c). Consistently, rapamycin ameliorated cisplatin-induced tubular damage in renal cortex and outer medulla, as indicated by histological examination (Figure 9d). The tubular damage score was 2.7 for the cisplatin group and 1.9 for the cisplatin + rapamycin group (Figure 9e). Together, these results suggest that enhancement of autophagy by rapamycin may protect against cisplatin-induced AKI, providing further support for the renoprotective role of autophagy in kidneys.

DISCUSSION

The role of autophagy in AKI remains controversial. Although we and others provided evidence for a renoprotective role of autophagy in AKI,[22–25] there are several reports supporting a role of autophagy in tubular cell death in the disease condition.[19–21] It is noteworthy that these studies mainly used *in vitro* cell culture models or *in vivo* models testing pharmacological autophagy inhibitors. The latest work by Kimura *et al.*[28] demonstrated heightened renal ischemia–reperfusion injury in proximal tubule–specific Atg5-knockout mice, providing the first *in vivo* genetic evidence for a renoprotective role in this AKI model. Our present study has used both pharmacologic and genetic approaches to determine the role of autophagy in ischemic, as well as cisplatin nephrotoxic, AKI. The results show that inhibition of autophagy by chloroquine or conditional Atg7 ablation from proximal tubules aggravates AKI, whereas activation of autophagy by rapamycin protects against AKI. Collectively, these *in vivo* pharmacological and conditional knockout studies have demonstrated the definitive evidence for a renoprotective role of autophagy in both ischemic and nephrotoxic AKI.

Conditional knockout of Atg7 in liver and brain affects development, anatomy, histology, and function of the organs and even life span of the animals.[14,37,38] Nevertheless, the renal proximal tubule–specific Atg7-knockout mice generated in our study were normal at birth and had no obvious developmental defects in kidneys. As suggested in our recent work,[39] owing to the late turn-on feature of the PEPCK promoter (3 weeks after birth), Cre is not expressed in proximal tubules until kidney development has mostly completed, which may explain the normal renal development in PT-Atg7-KO mice. At 8–10 weeks, the kidney tissues of PT-Atg7-KO mice were defective in clearance of protein aggregates, showing increased level of p62 and accumulation of cytoplasmic inclusion bodies (Figure 3). However, these mice showed little difference from their wild-type littermates on body weight, kidney weight/size, renal histology, and renal function within the age of up to 3 months (Figure 5 and data not shown). Autophagy defects due to Atg5 deletion in podocytes leads to glomerulopathy and proteinuria in aging mice.[18] Recent studies further demonstrated that Atg5 knockout from proximal tubules in mice results in tubular degeneration at late age.[28] It would be interesting to verify the effect of defective autophagy on aging kidneys in our PT-Atg7-KO model.

In our study, in addition to LC3, p62 was examined to monitor autophagy induction and flux. As a ubiquitin-binding protein, p62 is also a selective substrate of autophagy owing to its direct interaction with LC3 to facilitate autophagy degradation of ubiquitinated proteins.[40] Theoretically, the cellular level of p62 should inversely correlate with autophagy activity. This was true when wild-type and PT-Atg7-KO tissues were compared under unchallenged or control conditions, where PT-Atg7-KO tissues showed p62 accumulation (Figure 3c and d). However, following cisplatin treatment, autophagy induction in kidney tissues was not accompanied by p62 decrease, but instead, it accumulated (Figures 2a, 4a and d). The p62 accumulation was not caused by cessation of autolysosomal degradation, because autophagic flux during cisplatin treatment was efficient as indicated

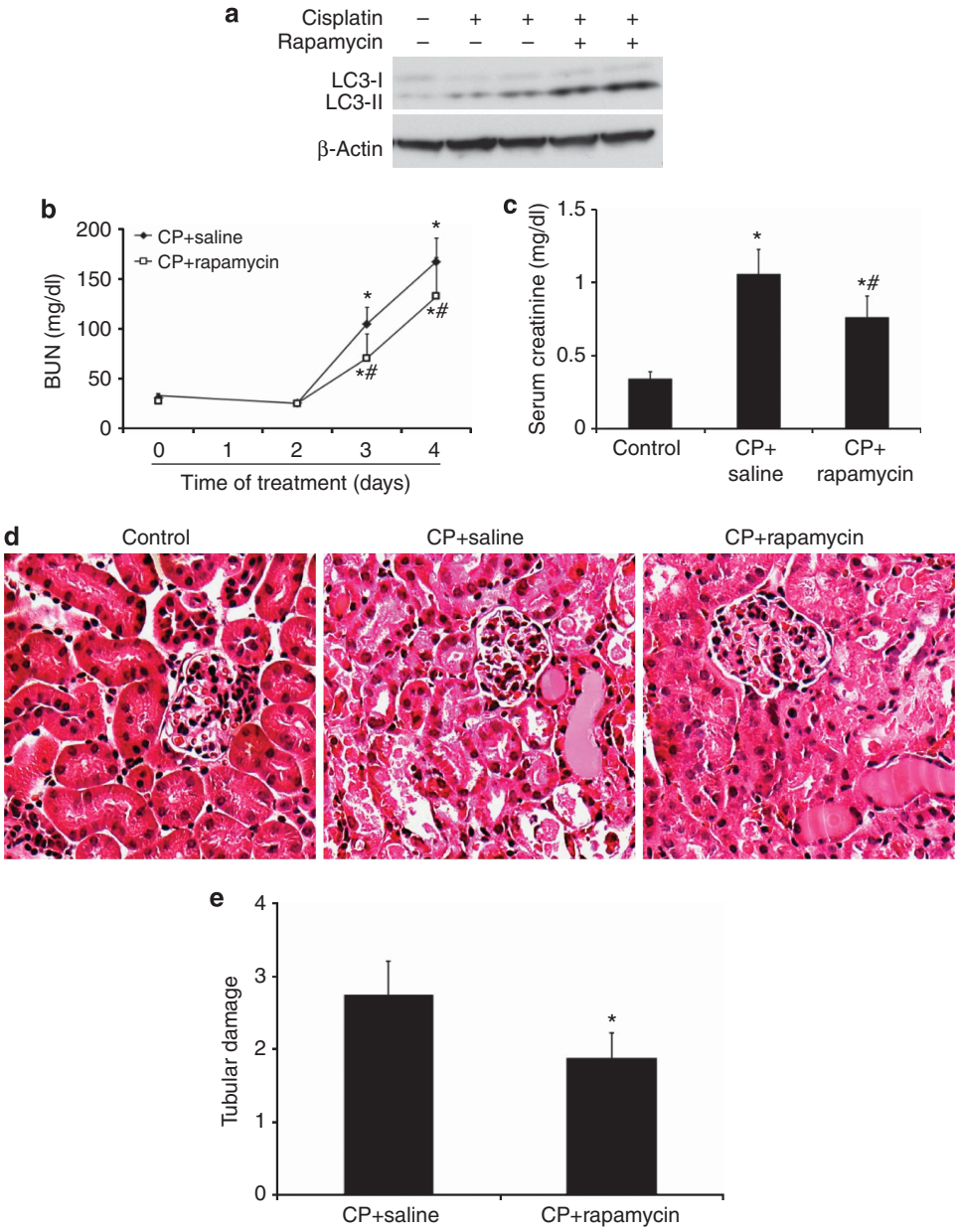

Figure 9 | Induction of autophagy by rapamycin reduces cisplatin-induced acute kidney injury (AKI) in C57BL/6 mice. C57BL/6 mice (male, 8–10 weeks old) were divided into three groups for the following treatments, respectively: (1) saline control ($n = 4$); (2) cisplatin + saline ($n = 12$); and (3) cisplatin + rapamycin ($n = 13$). (**a**) At 2 days after treatment, whole-tissue lysate of kidney cortex was collected for immunoblot analysis of LC3 and β-actin. (**b**, **c**) Blood samples were collected for measurements of blood urea nitrogen (BUN) and serum creatinine levels. Data are expressed as mean ± s.d. $^{*}P < 0.05$, significantly different from the control (or day 0) group; $^{\#}P < 0.05$, significantly different from the cisplatin + saline group. (**d**) Representative histology of kidney cortex (hematoxylin–eosin (H–E) staining, original magnification × 200). (**e**) Pathological score of tubular damage in cisplatin + saline and cisplatin + rapamycin groups. Data are expressed as mean ± s.d. $^{*}P < 0.05$, significantly different from the cisplatin + saline group.

by the effect of chloroquine that further increased LC3-II and p62 (Figure 2a). It is noteworthy that in immunohistochemistry cisplatin-induced p62 staining in wild-type tissues was different from that of PT-Atg7-KO tissues with impaired autophagy. In PT-Atg7-KO tissues, p62 accumulated as cytoplasmic inclusion bodies, whereas in wild-type tissues p62 staining was diffuse and not indicative of inclusion bodies (Figure 4d). Our interpretation is that p62 accumulation in PT-Atg7-KO tissues results from autophagic defects, whereas cisplatin-induced p62 accumulation in wild-type tissues may be a result of increased p62 expression and/or decreased proteasomal degradation of p62. It has been shown that p62 participates in proteasomal degradation, and its level may also increase when the proteasome pathway is inhibited.[41,42] In addition, p62 may be transcriptionally upregulated under certain conditions.[43]

The mechanism underlying the cytoprotective effect of autophagy remains unclear. Generally, we can envision several possibilities. (1) By digesting cellular constituents, autophagy generates substrates for ATP production and protein synthesis that are essential for adaptation to bioenergetic catastrophe. This occurs during cell starvation. This possibility is also relevant to ischemic and nephrotoxic AKI, where the availability of oxygen and nutrient has decreased and cells experience metabolic stress. (2) Autophagy is an important cellular housekeeping process that clears misfolded proteins, aggregates, and damaged organelles. This activity is particularly important for the cells under stress, in which protein misfolding and aggregation increase and cellular organelles are damaged. Removal of these potentially cytotoxic components by autophagy therefore provides a protective mechanism for cell survival. In this regard, damaged mitochondria and abnormal protein aggregates were shown in Atg5-knockout proximal tubular cells in mouse kidneys.[28] (3) Autophagy may interfere with or compromise the cell death signaling pathways. This possibility is best illustrated by the action of Beclin-1 (also called Atg6). Beclin-1 is a core protein in the complex of autophagy induction, but it also interacts with Bcl-2 (B-cell lymphoma 2), a well-known antiapoptotic protein. During autophagy, Beclin-1 moves into the autophagy induction complex and dissociates from Bcl-2, resulting in the release of Bcl-2 for cytoprotection.[44] Nevertheless, Beclin-1/Bcl-2 interaction was not verified during cisplatin treatment of renal tubular cells.[24] (4) Finally, recent studies have demonstrated that autophagy can negatively regulate inflammatory response, protecting cells from ischemic brain injury and endotoxin-induced intestinal epithelium injury *in vivo*.[45,46] In our present study, we have examined the effects of autophagy on p53 and mitogen-activated protein kinases, the two signaling pathways contributing to tubular cell apoptosis during cisplatin-AKI.[4,5,34] We demonstrated a heightened activation of p53 and JNK during cisplatin-AKI in PT-Atg7-KO tissues, which is consistent with the aggravated kidney injury in these animals (Figure 6). Interestingly, compared with wild-type kidneys, PT-Atg7-KO tissues had higher levels of both total and phosphorylated p38 kinase under control conditions. Following cisplatin treatment, p38 was phosphorylated and activated in wild-type tissues, but not in PT-Atg7-KO tissues. Further studies need to gain insights into the molecular mechanism whereby autophagy modulates these signaling pathways and protects cells and tissues in disease conditions such as AKI.

MATERIALS AND METHODS

PT-Atg7-KO mouse model was established by breeding $Atg7^{flox/flox}$ mice[14] with PEPCK-Cre transgenic mice obtained from Dr Volker Haase (University of Pennsylvania, Philadelphia, PA).[31] Genotyping was performed according to a modified protocol from Dr Zhenyu Yue (Mount Sinai School of Medicine, New York, NY) and our recent work.[39] Acute kidney injury was induced in mice by cisplatin and renal ischemia–reperfusion as previously described.[22,47] Primary proximal tubular cells were isolated from mouse kidneys and cultured as described previously.[36] Renal function, histology, immunohistochemistry, and apoptosis were examined using standard methods.[22,47] Detailed methods including statistical analysis are described in Supplementary Information online.

ACKNOWLEDGMENTS

We thank Dr Volker Haase at Vanderbilt University School of Medicine (Nashville, TN) for providing the PEPCK-Cre mouse line. We also thank Dr Zhenyu Yue at Mount Sinai School of Medicine (New York, NY) for providing the modified Atg7 genotyping protocol. The sources of support were National Institutes of Health and Department of Veterans Affairs of USA. During the revision of this manuscript, Takahashi *et al*.[48] reported that Atg5 knockout in proximal tubules enhanced cisplatin-induced AKI in mice, corroborating with the present study.

DISCLOSURE

All the authors declared no competing interests.

SUPPLEMENTARY MATERIAL

Supplementary material is linked to the online version of the paper at http://www.nature.com/ki

REFERENCES

1. Waikar SS, Curhan GC, Wald R *et al.* Declining mortality in patients with acute renal failure, 1988 to 2002. *J Am Soc Nephrol* 2006; **17**: 1143–1150.
2. Xue JL, Daniels F, Star RA *et al.* Incidence and mortality of acute renal failure in Medicare beneficiaries, 1992 to 2001. *J Am Soc Nephrol* 2006; **17**: 1135–1142.
3. Bonventre JV, Yang L. Cellular pathophysiology of ischemic acute kidney injury. *J Clin Invest* 2011; **121**: 4210–4221.
4. Pabla N, Dong Z. Cisplatin nephrotoxicity: mechanisms and renoprotective strategies. *Kidney Int* 2008; **73**: 994–1007.
5. Price PM, Safirstein RL, Megyesi J. The cell cycle and acute kidney injury. *Kidney Int* 2009; **76**: 604–613.
6. Sharfuddin AA, Molitoris BA. Pathophysiology of ischemic acute kidney injury. *Nat Rev Nephrol* 2011; **7**: 189–200.
7. Havasi A, Borkan SC. Apoptosis and acute kidney injury. *Kidney Int* 2011; **80**: 29–40.
8. Padanilam BJ. Cell death induced by acute renal injury: a perspective on the contributions of apoptosis and necrosis. *Am J Physiol Renal Physiol* 2003; **284**: F608–F627.
9. Borkan SC, Gullans SR. Molecular chaperones in the kidney. *Annu Rev Physiol* 2002; **64**: 503–527.
10. Lieberthal W. Macroautophagy: a mechanism for mediating cell death or for promoting cell survival? *Kidney Int* 2008; **74**: 555–557.
11. Periyasamy-Thandavan S, Jiang M, Schoenlein P *et al.* Autophagy: molecular machinery, regulation, and implications for renal pathophysiology. *Am J Physiol Renal Physiol* 2009; **297**: F244–F256.
12. Levine B, Klionsky DJ. Development by self-digestion: molecular mechanisms and biological functions of autophagy. *Dev Cell* 2004; **6**: 463–477.
13. Mizushima N, Yoshimori T, Ohsumi Y. The role of atg proteins in autophagosome formation. *Annu Rev Cell Dev Biol* 2011; **27**: 107–132.
14. Komatsu M, Waguri S, Ueno T *et al.* Impairment of starvation-induced and constitutive autophagy in Atg7-deficient mice. *J Cell Biol* 2005; **169**: 425–434.
15. Baehrecke EH. Autophagy: dual roles in life and death? *Nat Rev* 2005; **6**: 505–510.
16. Maiuri MC, Zalckvar E, Kimchi A *et al.* Self-eating and self-killing: crosstalk between autophagy and apoptosis. *Nat Rev* 2007; **8**: 741–752.
17. Mizushima N, Levine B, Cuervo AM *et al.* Autophagy fights disease through cellular self-digestion. *Nature* 2008; **451**: 1069–1075.
18. Hartleben B, Godel M, Meyer-Schwesinger C *et al.* Autophagy influences glomerular disease susceptibility and maintains podocyte homeostasis in aging mice. *J Clin Invest* 2010; **120**: 1084–1096.
19. Chien CT, Shyue SK, Lai MK. Bcl-xL augmentation potentially reduces ischemia/reperfusion induced proximal and distal tubular apoptosis and autophagy. *Transplantation* 2007; **84**: 1183–1190.
20. Suzuki C, Isaka Y, Takabatake Y *et al.* Participation of autophagy in renal ischemia/reperfusion injury. *Biochem Biophys Res Commun* 2008; **368**: 100–106.

21. Inoue K, Kuwana H, Shimamura Y *et al.* Cisplatin-induced macroautophagy occurs prior to apoptosis in proximal tubules *in vivo*. *Clin Exp Nephrol* 2010; **14**: 112–122.
22. Jiang M, Liu K, Luo J *et al.* Autophagy is a renoprotective mechanism during *in vitro* hypoxia and *in vivo* ischemia-reperfusion injury. *Am J Pathol* 2010; **176**: 1181–1192.
23. Pallet N, Bouvier N, Legendre C *et al.* Autophagy protects renal tubular cells against cyclosporine toxicity. *Autophagy* 2008; **4**: 783–791.
24. Periyasamy-Thandavan S, Jiang M, Wei Q *et al.* Autophagy is cytoprotective during cisplatin injury of renal proximal tubular cells. *Kidney Int* 2008; **74**: 631–640.
25. Yang C, Kaushal V, Shah SV *et al.* Autophagy is associated with apoptosis in cisplatin injury to renal tubular epithelial cells. *Am J Physiol Renal Physiol* 2008; **294**: F777–F787.
26. Bolisetty S, Traylor AM, Kim J *et al.* Heme oxygenase-1 inhibits renal tubular macroautophagy in acute kidney injury. *J Am Soc Nephrol* 2011; **21**: 1702–1712.
27. Li L, Zepeda-Orozco D, Black R *et al.* Autophagy is a component of epithelial cell fate in obstructive uropathy. *Am J Pathol* 2010; **176**: 1767–1778.
28. Kimura T, Takabatake Y, Takahashi A *et al.* Autophagy protects the proximal tubule from degeneration and acute ischemic injury. *J Am Soc Nephrol* 2011; **22**: 902–913.
29. Wei Q, Dong G, Franklin J *et al.* The pathological role of Bax in cisplatin nephrotoxicity. *Kidney Int* 2007; **72**: 53–62.
30. Ohsumi Y, Mizushima N. Two ubiquitin-like conjugation systems essential for autophagy. *Semin Cell Dev Biol* 2004; **15**: 231–236.
31. Rankin EB, Tomaszewski JE, Haase VH. Renal cyst development in mice with conditional inactivation of the von Hippel-Lindau tumor suppressor. *Cancer Res* 2006; **66**: 2576–2583.
32. Komatsu M, Waguri S, Koike M *et al.* Homeostatic levels of p62 control cytoplasmic inclusion body formation in autophagy-deficient mice. *Cell* 2007; **131**: 1149–1163.
33. Ramesh G, Reeves WB. Inflammatory cytokines in acute renal failure. *Kidney Int Suppl* 2004; **66**: S56–S61.
34. Jiang M, Dong Z. Regulation and pathological role of p53 in cisplatin nephrotoxicity. *J Pharmacol Exp Ther* 2008; **327**: 300–307.
35. Jiang M, Wei Q, Wang J *et al.* Regulation of PUMA-alpha by p53 in cisplatin-induced renal cell apoptosis. *Oncogene* 2006; **25**: 4056–4066.
36. Wei Q, Dong G, Yang T *et al.* Activation and involvement of p53 in cisplatin-induced nephrotoxicity. *Am J Physiol Renal Physiol* 2007; **293**: F1282–F1291.
37. Komatsu M, Waguri S, Chiba T *et al.* Loss of autophagy in the central nervous system causes neurodegeneration in mice. *Nature* 2006; **441**: 880–884.
38. Komatsu M, Wang QJ, Holstein GR *et al.* Essential role for autophagy protein Atg7 in the maintenance of axonal homeostasis and the prevention of axonal degeneration. *Proc Natl Acad Sci USA* 2007; **104**: 14489–14494.
39. Wei Q, Bhatt K, He HZ *et al.* Targeted deletion of Dicer from proximal tubules protects against renal ischemia-reperfusion injury. *J Am Soc Nephrol* 2010; **21**: 756–761.
40. Bjorkoy G, Lamark T, Brech A *et al.* p62/SQSTM1 forms protein aggregates degraded by autophagy and has a protective effect on huntingtin-induced cell death. *J Cell Biol* 2005; **171**: 603–614.
41. Bardag-Gorce F, Francis T, Nan L *et al.* Modifications in P62 occur due to proteasome inhibition in alcoholic liver disease. *Life Sci* 2005; **77**: 2594–2602.
42. Kuusisto E, Suuronen T, Salminen A. Ubiquitin-binding protein p62 expression is induced during apoptosis and proteasomal inhibition in neuronal cells. *Biochem Biophys Res Commun* 2001; **280**: 223–228.
43. Nakaso K, Yoshimoto Y, Nakano T *et al.* Transcriptional activation of p62/A170/ZIP during the formation of the aggregates: possible mechanisms and the role in Lewy body formation in Parkinson's disease. *Brain Res* 2004; **1012**: 42–51.
44. Wei Y, Pattingre S, Sinha S *et al.* JNK1-mediated phosphorylation of Bcl-2 regulates starvation-induced autophagy. *Mol Cell* 2008; **30**: 678–688.
45. Zhou X, Zhou J, Li X *et al.* GSK-3beta inhibitors suppressed neuroinflammation in rat cortex by activating autophagy in ischemic brain injury. *Biochem Biophys Res Commun* 2011; **411**: 271–275.
46. Fujishima Y, Nishiumi S, Masuda A *et al.* Autophagy in the intestinal epithelium reduces endotoxin-induced inflammatory responses by inhibiting NF-kappaB activation. *Arch Biochem Biophys* 2011; **506**: 223–235.
47. Brooks C, Wei Q, Cho S *et al.* Regulation of mitochondrial dynamics in acute kidney injury in cell culture and rodent models. *J Clin Invest* 2009; **119**: 1275–1285.
48. Takahashi A, Kimura T, Takabatake Y *et al.* Autophagy guards against cisplatin-induced acute kidney injury. *Am J Pathol* 2012; **180**: 517–525.